Original Article

Predicting therapeutic responses in head and neck squamous cell carcinoma from *TP53* mutation detected by cell-free DNA

Mei Wei[1,2,3,4,5], Jingtai Zhi[1,2,3,4,5], Li Li[1,2,3,4,5], Wei Wang[1,2,3,4,5]

[1]Department of Otorhinolaryngology Head and Neck Surgery, Tianjin First Central Hospital, Tianjin, China; [2]Institute of Otolaryngology of Tianjin, Tianjin First Central Hospital, Tianjin, China; [3]Key Laboratory of Auditory Speech and Balance Medicine, Tianjin First Central Hospital, Tianjin, China; [4]Key Clinical Discipline of Tianjin (Otolaryngology), Tianjin First Central Hospital, Tianjin, China; [5]Otolaryngology Clinical Quality Control Centre, Tianjin First Central Hospital, Tianjin, China

Contributions: (I) Conception and design: W Wang, M Wei; (II) Administrative support: W Wang, L Li; (III) Provision of study materials or patients: J Zhi, L Li; (IV) Collection and assembly of data: M Wei, J Zhi; (V) Data analysis and interpretation: W Wang; (VI) Manuscript writing: All authors; (VII) Final approval of manuscript: All authors.

Correspondence to: Wei Wang, MD. Department of Otorhinolaryngology Head and Neck Surgery, Tianjin First Central Hospital, Tianjin, China; Institute of Otolaryngology of Tianjin, Tianjin First Central Hospital, Tianjin, China; Key Laboratory of Auditory Speech and Balance Medicine, Tianjin First Central Hospital, Tianjin, China; Key Clinical Discipline of Tianjin (Otolaryngology), Tianjin First Central Hospital, Tianjin, China; Otolaryngology Clinical Quality Control Centre, Tianjin First Central Hospital, No. 24 Fukang Road, Nankai District, Tianjin, China. Email: entwangwei@nankai.edu.cn.

Background: Head and neck squamous cell carcinoma (HNSCC) is an epithelial malignant tumor originating from the oral cavity, oropharynx, nasal cavity, sinuses, nasopharynx, hypopharynx, or larynx. Mutations in *TP53* are the most common of all somatic genomic changes in HNSCC, and *TP53* mutations are associated with the response to immunotherapy and chemotherapy. Tumor-derived circulating cell-free DNA (cfDNA) is a minimally invasive method to determining genetic alterations in cancer. This study aimed to explore the therapeutic responses of patients with HNSCC with *TP53* mutation and the accuracy of cfDNA for detecting *TP53* mutation.

Methods: Information on *TP53* mutations, patient survival time, and clinical data in HNSCC were downloaded from The Cancer Genome Atlas database. The difference in immune infiltration between the *TP53*-mutant group and the wild-type group was compared. We applied the single-sample gene set enrichment analysis method on the transcriptome of HNSCC samples to assess the distribution of immune cell types between the two groups. The chemotherapy response was constructed using the R software package, "pRRophetic". Gene set enrichment analysis was performed based on the *TP53* mutation. The next-generation sequencing was executed on cfDNA from nine patients with HNSCC to detect genetic alterations. Tumor biopsy (n=9) was sequenced using the same technique.

Results: *TP53* was the most frequently mutated gene in HNSCC. The *TP53* mutation was related to immune cells and the expression of immune-associated genes. The *TP53* mutation group showed lower response to immunotherapy but high sensitivity to some chemotherapies compared with the wild-type group. *TP53* was the most frequently mutated gene (6/9; 66.67%) in cfDNA. Only 27.27% of *TP53* mutations in tumor tissue were detected outside of cfDNA.

Conclusions: *TP53* mutation could be used as a specific predictor of treatment response in patients with HNSCC. Using cfDNA to detect the *TP53* mutations in patients with HSNCC is a feasible method. The results suggested that the therapeutic response in patients could be predicted by detecting *TP53* mutations in cfDNA, and large-scale and prospective studies are needed to validate this hypothesis.

Keywords: *TP53* mutations; head and neck squamous cell carcinoma (HNSCC); immunotherapy; chemotherapy; cell-free DNA (cfDNA)

Submitted May 22, 2023. Accepted for publication Oct 08, 2023. Published online Dec 11, 2023.
doi: 10.21037/tcr-23-878
View this article at: https://dx.doi.org/10.21037/tcr-23-878

Introduction

Head and neck squamous cell carcinoma (HNSCC) is one of the most common cancers in humans. More than 600,000 new cases of HNSCC worldwide are recorded each year, and of these cases, approximately 355,000 result in death (1). Smoking, human papillomavirus (HPV) infection, and alcohol consumption are the most significant risk factors for HNSCC (2). Tumor-suppressor *TP53* mutation is the most frequently mutated gene in HNSCC, and it is present in approximately 70% of cases, although the frequency varies in different head and neck regions (3). Different *TP53* mutations may have varying gain-of-function characteristics. The loss of p53 function would weaken the activation of cell cycle checkpoints and cell apoptosis, thereby resulting in the acquisition of additional mutations and gradual accumulation of a significant tumor mutation burden (4). *TP53* mutations are closely associated with adverse outcomes and treatment options in HNSCC.

Cell-free DNA (cfDNA), as a biomarker of blood, has attracted considerable attention for its potential as a minimally invasive tool for cancer monitoring (5,6). Apoptosis, necrosis, and the release of viable cells with newly synthesized DNA are major sources of cfDNA (7,8). Quantification of nontumor-specific and tumor-derived cfDNA and the presence of genetic and epigenetic variants in cfDNA are potential biomarkers of cancer.

Highlight box

Key findings

- Cell-free DNA (cfDNA) can detect *TP53* mutations in patients and predict their immune therapy response and prognosis.

What is known and what is new?

- *TP53* mutation in patients with head and neck squamous cell carcinoma (HNSCC) is known to lead to poor prognosis.
- In our study, we found that patients with HSNCC with *TP53* mutations had poor response to immunotherapy and chemotherapy. Additionally, cfDNA can be used to detect *TP53* mutations in patients.

What is the implication, and what should change now?

- In the future, cfDNA, a noninvasive detection method, can be used to detect *TP53* mutations and predict patient treatment responses.

In this study, we investigated the association of *TP53* mutation with the prognosis of patients with HNSCC from The Cancer Genome Atlas (TCGA) dataset. Furthermore, we investigated whether the *TP53* mutation is associated with immunotherapy and chemotherapeutic responses. Ultimately, we found that the presence of *TP53* mutations could be detected by cfDNA. It may be possible to predict the response to immunotherapy and chemotherapy for patients with HSNCC by detecting *TP53* mutations in cfDNA. We present this article in accordance with the REMARK reporting checklist (available at https://tcr.amegroups.com/article/view/10.21037/tcr-23-878/rc).

Methods

Data acquisition and analysis

We downloaded information on HNSCC gene expression profiles, clinical profile, and *TP53* mutations from TCGA database (http://xena.ucsc.edu/). Level 4 transcriptomic and reverse-phase protein array (RPPA) data of patients with cancer were obtained from TCGA. Correlation analysis was performed using the expression of genes extracted from the corresponding packages in R software (The R Foundation of Statistical Computing). The masked somatic mutation data were summarized and visualized with R software "Maftools".

Estimating immune cell infiltration

To verify differences in immunity between the *TP53* mutation and wild-type groups, the "estimate" package for R was used to calculate the stromal score, immune score, and ESTIMATE score. Meanwhile, the single-sample gene set enrichment analysis (ssGSEA) algorithm was employed to evaluate the immune cells in the HNSCC samples from gene expression data.

Immunotherapeutic and chemotherapeutic response prediction

The tumor immune dysfunction and exclusion (TIDE) can be used to evaluate the possibility of tumor immune escape

in the gene expression profile of tumor samples (9). In this study, TIDE was used to calculate immune measures of HNSCC (http://tide.dfci.harvard.edu). The "pRRophetic" R package was used to predict the chemotherapy response as quantified by the median maximum inhibitory concentration (IC_{50}) for each patient with HNSCC (10,11).

Gene Ontology (GO) analysis, Kyoto Encyclopedia of Genes and Genomes (KEGG) database analysis, and GSEA

Differentially expressed genes (DEGs) between patients with and without *TP53* mutations in the HNSCC cohort were obtained using the "limma" package in R. According to the following significance standard, 403 DEGs with | log fold change | >1 and false-discovery rate (FDR) <0.05 were selected. The "pheatmap" R package was used to generate a heatmap plot to visualize the DEGs. GO functional annotation and KEGG pathway enrichment analyses were conducted using R software packages "clusterProfiler", "org.Hs.eg.db", "enrichplot", and "ggplot2". GSEA was performed to identify the signaling pathways wherein DEGs were enriched between the 2 subgroups (12).

Detection of mutations in plasma DNA

The study was conducted in accordance with the Declaration of Helsinki (as revised in 2013) and was approved by the independent ethics committee of Tianjin First Central Hospital, China (protocol no. 2020N115KY). Informed consent was obtained from all individual participants. Patients histopathologically diagnosed with HNSCC were recruited into the study. The clinical investigations, including of tumor size, lymph node involvement and any evidence of metastasis, and clinical tumor node metastasis (TNM) staging, were performed in accordance with the American Joint Committee on Cancer Manual of Head and Neck Cancer Staging, eighth edition (13). Patients who received any treatment or had a history of other malignancies were excluded. Before participating in the study, patients who enrolled in Tianjin First Central Hospital agreed on the use of their tissue, blood samples, and data. Collected tissue and plasma samples were stored in a –80 ℃ freezer for later examination.

Steps for mutation detection in cfDNA: (I) DNA sample testing: cfDNA was extracted from the patient's plasma as a tumor sample, and the peripheral blood mononuclear cells (PBMCs) of the patient were selected as the normal control. A Qubit 2.0 fluorometer (Thermo Fisher Scientific, USA) was used to measure the sample concentration, and Agilent 2100 bioanalyzer (Agilent Technologies, Inc., USA) was used to detect the sample fragment size. cfDNA samples with DNA concentrations ≥20 ng/μL, total amounts of more than 20–30 ng, and no genomic pollution were used to build the database. (II) Library construction: As most cfDNA samples were small fragments of approximately 170 bp and there was a small number of fragments of 170-bp integer multiples, the biggest difference between cfDNA samples and nucleic acid samples was that the cfDNA samples did not need to be randomly broken into small fragments by a Covaris crusher. After end repair, phosphorylation, and A-tail addition, the ends of the fragments were connected to connectors to prepare a DNA library. (III) Library detection: After the construction of the library, the Qubit 2.0 fluorometer was first used for preliminary quantification, and then the Agilent 2100 was bioanalyzer was used to detect the insert size of the library. After the insert size was found to meet expectations 170 bp, quantitative polymerase chain reaction (qPCR) was applied to accurately quantify the effective concentration (3 nmol/L) of the library to ensure library quality. Given that cfDNA was a special sample, its fragment size was 170 bp, and its integer was multiple, the target fragment with an insert size of approximately 170 bp was selected for subsequent sequencing through purification. (IV) Computer sequencing: after the library inspection was qualified, sequencing with a NovaSeq system (Illumina, USA) with pair end 150 bp (PE150) was conducted according to the effective concentration of the library and the data output demand. In the constructed small fragment library, insert DNA, that was, insert fragments, was considered to be the unit of high-throughput and direct sequencing. Double-ended sequencing was used a method for sequencing the two ends of each inserted segment. The length distribution of inserted fragments was known so that the sequences at both ends of the fragments could be determined, and the length between the two fragments was also known during the double-ended sequencing process for subsequent comparison and analysis.

Study design

A retrospective analysis method was used to analyze the *TP53* mutation status in patients with HSNCC, as well as the impact of *TP53* mutations on patient survival, immunity, and chemotherapy response. In addition, gene mutations

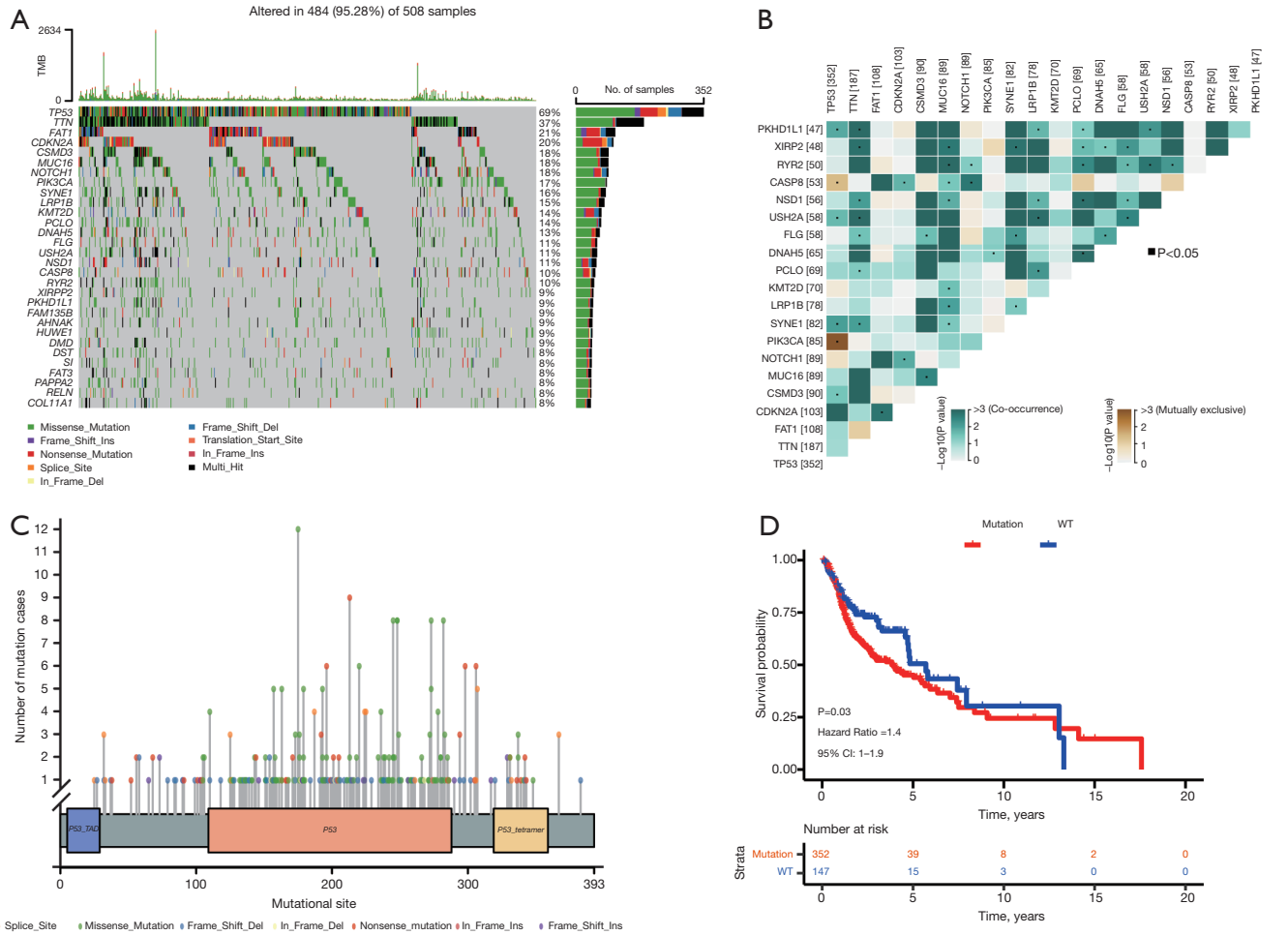

Figure 1 Somatic genome mutations in HNSCC, as well as *TP53* mutations and their impact on survival. (A) Waterfall plot of commonly mutated genes in HNSCC in TCGA cohort; (B) the coincident and exclusive associations across mutated genes; (C) Lollipop map showing the location and type of *TP53* mutations in HNSCC; (D) effect of Kaplan-Meier survival curve of *TP53* mutation on survival. HNSCC, head and neck squamous cell carcinoma; TCGA, The Cancer Genome Atlas; TMB, tumor mutational burden; WT, wild type.

that could be detected in patients' cfDNA and tissues were compared. We explored the feasibility of using cfDNA in blood as a noninvasive detection method to detect *TP53* mutations in patients.

Statistical analysis

The statistical analyses in this study were performed with R software version 4.1.3. One-way analysis of variance (ANOVA) was used to evaluate the relationship of *TP53* mutation and the clinical characteristics of HNSCC. In all analyses, statistical significance (α value) was set to 0.05, and all P values were two-sided.

Results

Somatic genomic mutations in HNSCC

We identified 30 frequently mutated genes using the HNSCC cohort in TCGA, and the 10 most frequently mutated genes were *TP53* (69%), *TTN* (37%), *FAT1* (21%), *CDKN2A* (20%), *CSMD3* (18%), *MUC16* (18%), *NOTCH1* (18%), *PIK3CA* (17%), *SYNE1* (16%), and *LRP1B* (15%) (*Figure 1A*). *TP53* was the most frequently mutated gene in HNSCC. We explored concordance and exclusivity relationships between the mutant genes shown in *Figure 1B*. *Figure 1C* is a lollipop plot drawn by Maftools, which shows the mutation distribution of *TP53* in HNSCC. The results

Table 1 Correlations between *TP53* mutation and clinicopathological characteristics

Parameter	*TP53* mutation	*TP53*-WT	χ^2 value	P value
Age			4.279	0.041
≤60 years	164	84		
>60 years	193	66		
Gender			0.113	0.827
Female	98	39		
Male	259	111		
M stage			0.226	>0.99
M0	335	142		
M1	4	1		
Missing value	18	7		
N stage			4.550	0.037
N0	179	61		
N1 + N2	161	84		
Missing value	17	5		
T stage			12.448	<0.001
T1 + T2	108	70		
T3 + T4	238	76		
Missing value	11	4		
Clinical stage			0.158	0.727
I + II	79	36		
III + IV	267	111		
Missing value	11	3		
Tumor grade			10.780	0.002
G1 + G2	275	90		
G3 + G4	73	49		
Missing value	9	11		

WT, wild type.

indicated that the majority of *TP53* mutations were missense mutations. The effect of *TP53* mutation on overall survival (OS) prognosis was assessed according to the Kaplan-Meier survival curve, and *TP53* mutation was found to be a poor prognostic factor for OS. Our result was consistent with previous reports (14,15) (*Figure 1D*). We then further analyzed *TP53* mutations in subsequent analyses.

Correlation between the TP53 mutation and clinicopathologic characteristics

This study included 507 patients, 357 of whom had *TP53* mutations, with the other 150 having the wild type. As shown in *Table 1*, the clinical characteristics of gender, clinical stage, and pathologic M (pM) showed no significant differences between the *TP53*-mutation and wild-type groups. Meanwhile, the clinical characteristics of age (χ^2=4.279; P=0.041), pathologic N stage (χ^2=4.550; P=0.037), pathologic T stage (χ^2=12.448; P<0.001), and tumor grade (χ^2=10.780; P=0.002) showed significant differences between the two groups.

Immune cell infiltration landscape of TP53 mutation in HNSCC

We performed an ESTIMATE analysis of the immune properties of *TP53* mutations based on the expression of immune cell types. The results revealed significant differences in immune (*Figure 2A*) and ESTIMATE scores (*Figure 2B*) but not in stromal scores (*Figure 2C*) between the two groups. The ssGSEA method was applied to the transcriptome of HNSCC samples to assess the distribution of immune cell types. Immune infiltration in patients in the *TP53*-mutant and wild-type groups was then elucidated. As shown in *Figure 2D*, more than half of the immune cell types were downregulated in the *TP53*-mutant group compared with the wild-type group. We observed significantly reduced levels of activated B cells, activated CD4 T cells, activated CD8 T cells, and eosinophils in the *TP53*-mutant group. CD56 bright natural killer (NK) cells were upregulated in the *TP53*-mutant group.

The TP53 mutation was associated with the expression of immune checkpoints

The expression of programmed cell death-ligand 1 (PD-L1) is widely recognized as a reliable biomarker for guiding the administration of immune checkpoint inhibitors (ICIs). To explore the role of *TP53* mutation in determining the response to ICIs, we performed several analyses to determine the association between *TP53* mutation and PD-L1 expression. PD-L1 (CD274) messenger RNA (mRNA) expression in the *TP53*-mutant group was significantly lower than that in the wild-type *TP53* group (P<0.01) (*Figure 3A*). This result was further confirmed at the PD-L1 protein level by RPPA data, and *TP53* mutation was associated with a lower PD-L1 protein level than was wild-type *TP53* (P<0.05) (*Figure 3B*). We also compared programmed cell death protein 1 (PD-1) and p53 expression levels in each *TP53* group. Compared with the wild-type group, the expression of p53 protein in the *TP53*-mutant group increased (*Figure 3C*), but no significant difference in

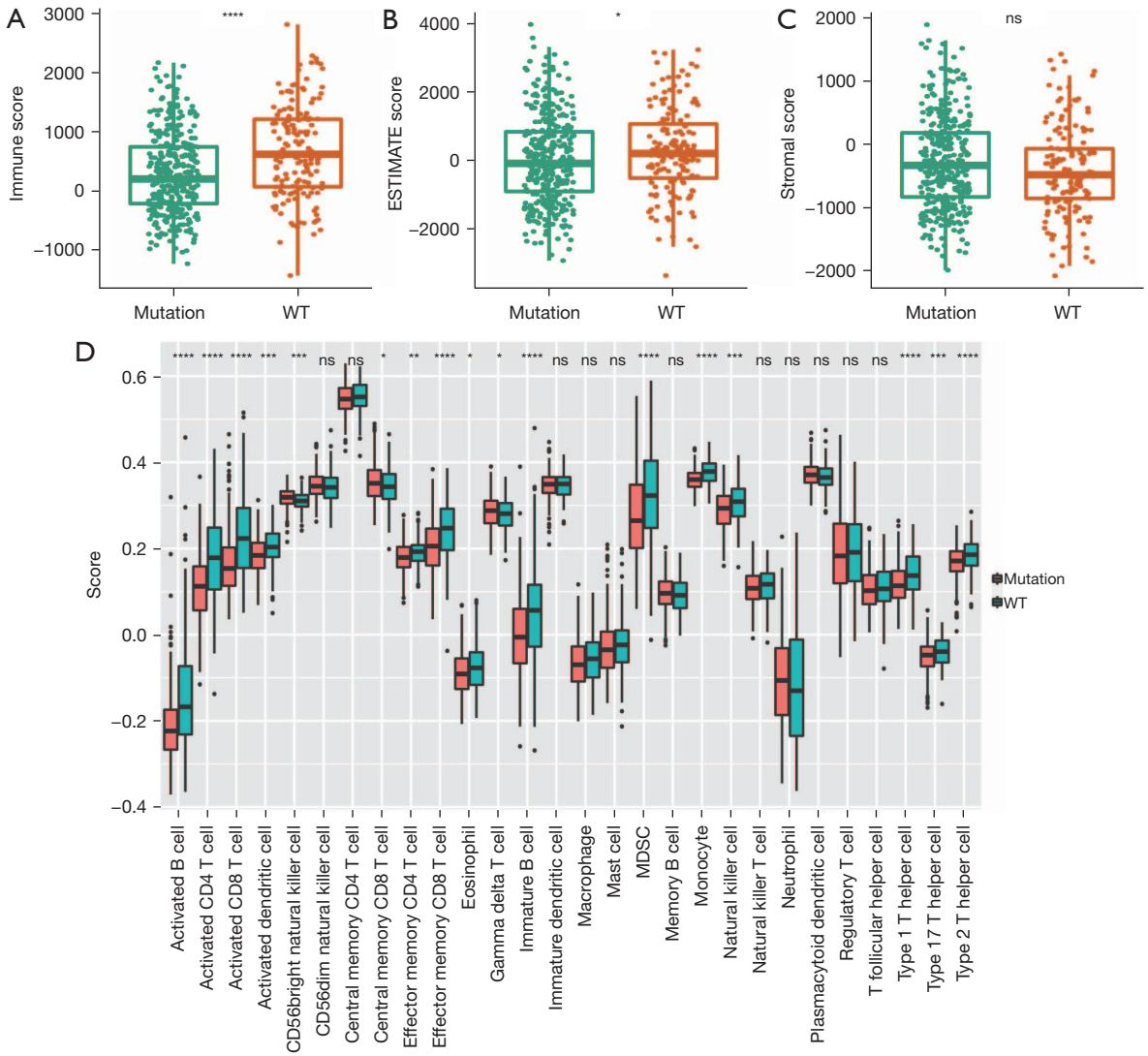

Figure 2 Immune cell infiltration in HNSCC. (A-C) Analysis of the immune score, ESTIMATE score, and stromal score between the *TP53*-mutant group and the wild-type group based on TCGA database; (D) differences in the distribution of immune cells between the *TP53*-mutant group and wild-type group based on TCGA database. *, P<0.05; **, P<0.01; ***, P<0.005; ****, P<0.001; ns, P>0.05. HNSCC, head and neck squamous cell carcinoma; TCGA, The Cancer Genome Atlas.

PD-1 levels between the groups was observed (*Figure 3D*).

Previous studies have shown that *TP53* mutation prevents HNSCC from downregulating PD-L1 expression via miR-34 (16,17). Therefore, the expression of miR-34 family members in the *TP53*-mutant group and the wild-type group was compared. The results showed that miR-34a was significantly decreased in the *TP53*-mutant group, and no significant difference was found for miR-34b or miR-34c (*Figure 3E-3G*), suggesting that the *TP53* mutation may not reduce PD-L1 levels through miR-34 regulation in HNSCC.

We also explored the expression of other immune checkpoints in *TP53* mutation, including cytotoxic t-lymphocyte associated protein 4 (CTLA-4), lymphocyte activation gene 3 (LAG3), galectin 9 (LGALS9), hepatitis a virus cellular receptor 2 (HAVCR2), programmed cell death 1 ligand 2 (PDCD1LG2), and T cell immunoreceptor with Ig and ITIM domains (TIGIT). We found that the expression levels of CTLA-4, LAG3, LGALS9, HAVCR2, and TIGIT were significantly reduced in *TP53*-mutant

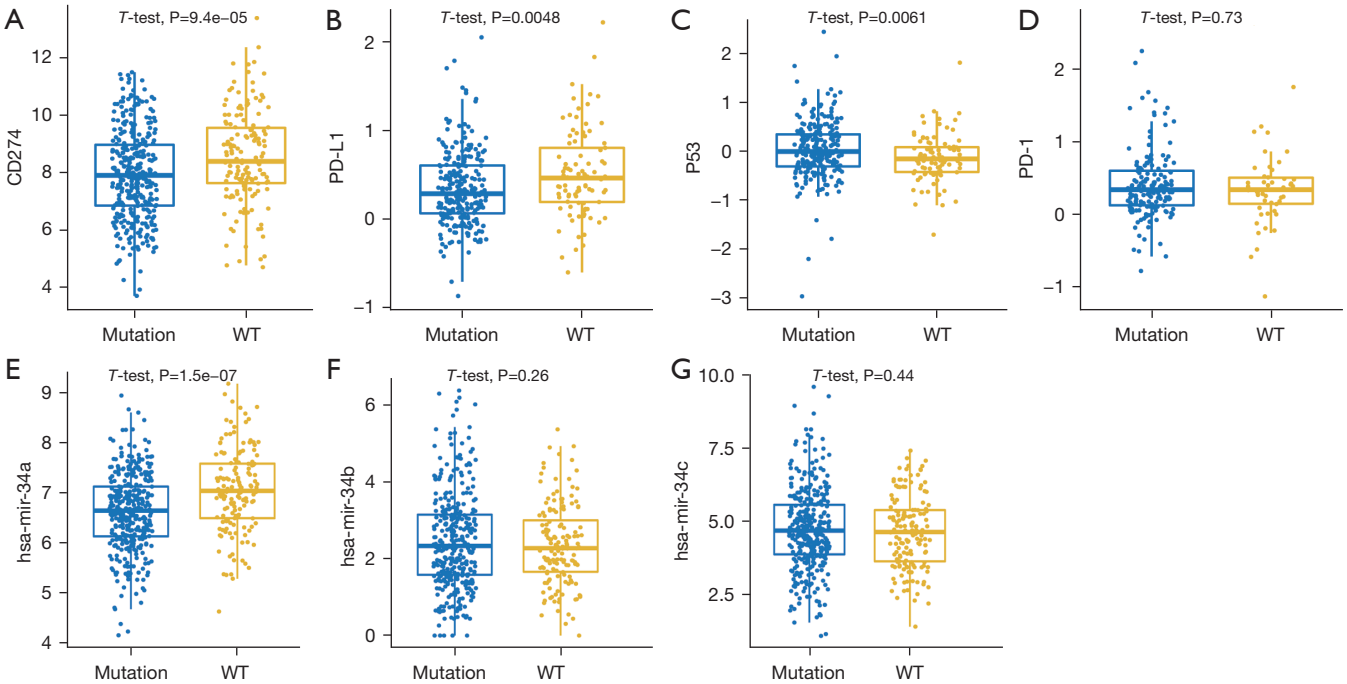

Figure 3 The relationship between *TP53* mutation and immune checkpoint expression level in HNSCC. (A,B) Correlation analysis of *TP53* status with PD-L1 mRNA and PD-L1 RPPA levels based on TCGA database; (C,D) correlation of *TP53* status with PD-1 and p53 RPPA levels; (E-G) correlation of *TP53* status with miR-34 family levels. HNSCC, head and neck squamous cell carcinoma; PD-L1, programmed cell death-ligand 1; RPPA, reverse-phase protein array; WT, wild-type.

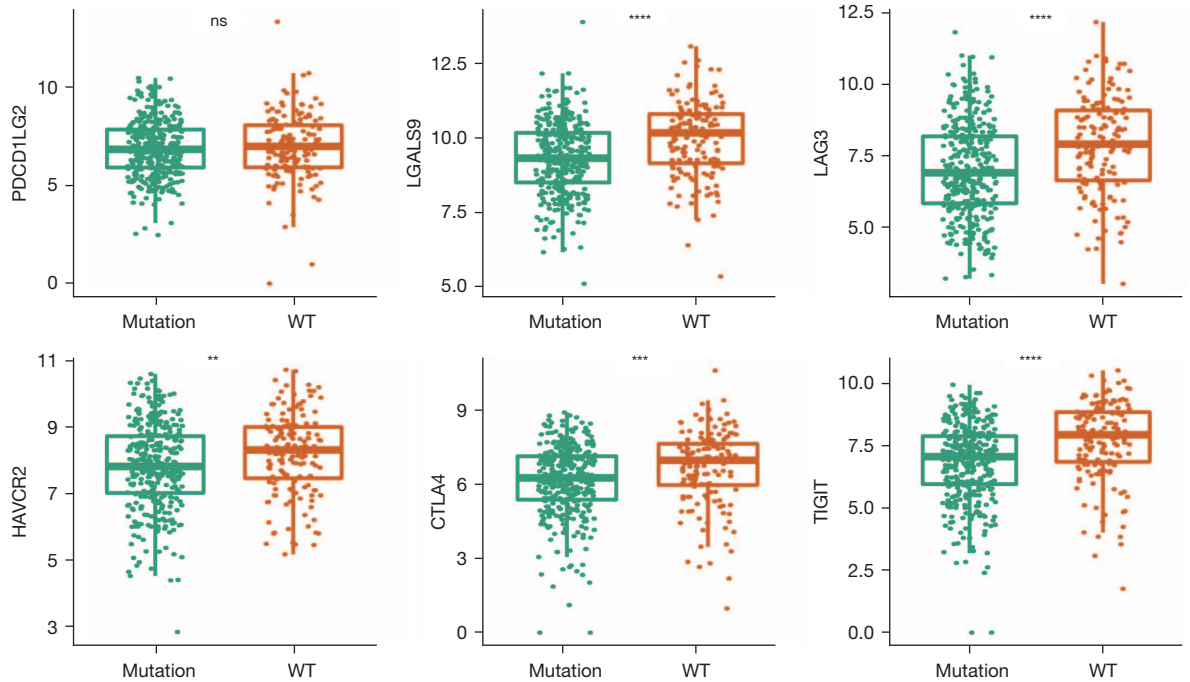

Figure 4 Differences in immune checkpoint–associated genes between *TP53* mutation and wild-type patients in HNSCC. **, P<0.01; ***, P<0.005; ****, P<0.001; ns, P>0.05. HNSCC, head and neck squamous cell carcinoma; WT, wild-type.

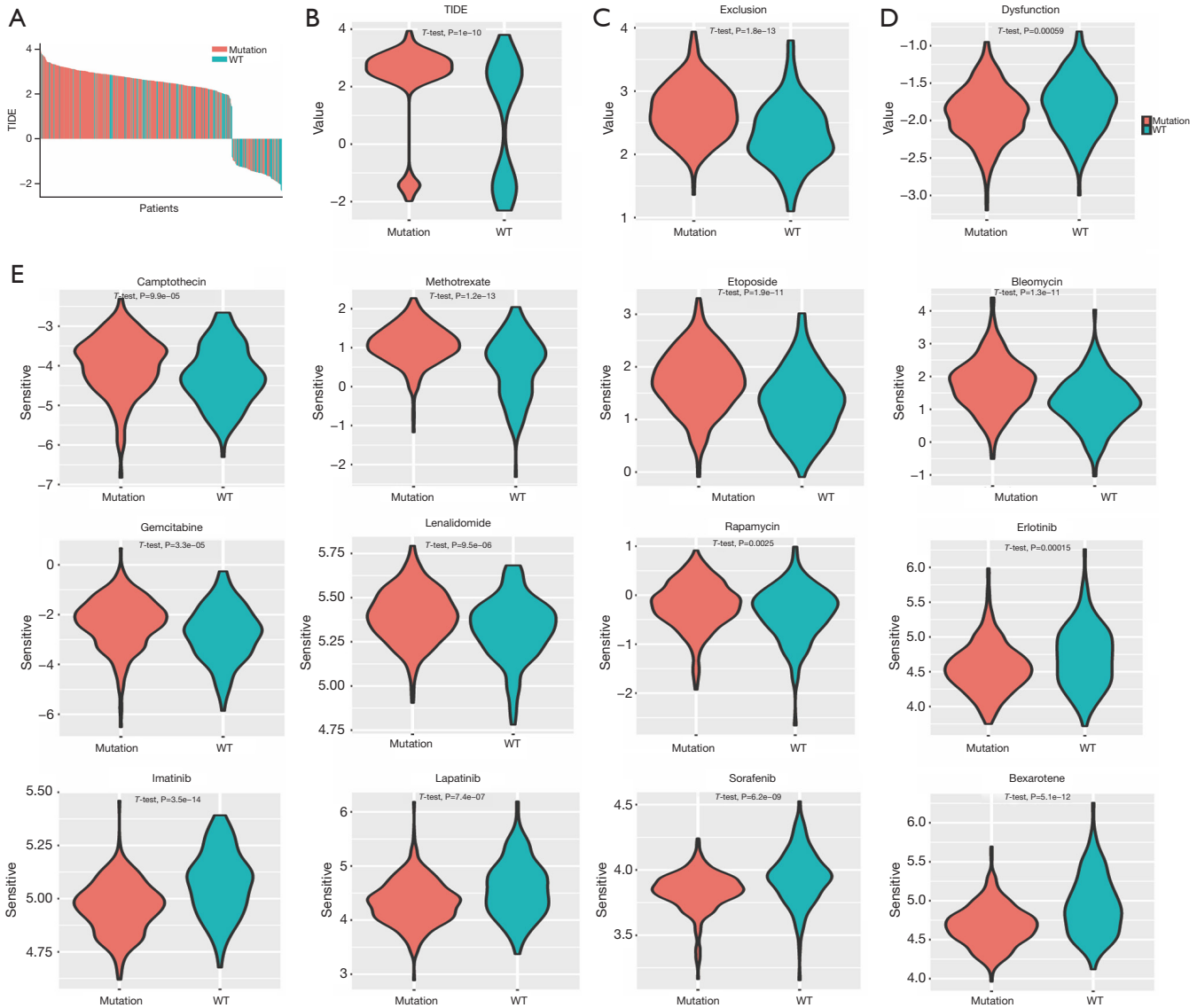

Figure 5 Immunotherapy and chemotherapy response in patients with HNSCC with mutant and wild-type *TP53* based on TCGA database. (A-D) Violin plot of different prediction scores of TIDE, together with the dysfunction score and exclusion score in the two groups. (E) Drugs with significantly different chemotherapy response (P<0.001) in the HNSCC test. WT, wild-type; TIDE, tumor immune dysfunction and exclusion; HNSCC, head and neck squamous cell carcinoma; TCGA, The Cancer Genome Atlas.

patients with HSNCC (*Figure 4*). These results suggested that immunotherapy that targets immune checkpoints might be less effective for patients with the *TP53* mutation.

Immunotherapeutic and chemotherapeutic responses of patients with TP53-mutant or TP53 wild-type HNSCC

To investigate the relationship between *TP53* mutation and ICI response in HNSCC, the TIDE algorithm was used to estimate the potential clinical efficacy of immune checkpoint blockade (ICB) therapy. The *TP53*-mutant group had a higher TIDE score (P<0.01; *Figure 5A*,*5B*), composed of higher TIDE exclusion scores (P<0.01; *Figure 5C*) and lower TIDE dysfunction signatures (P<0.01; *Figure 5D*). Our findings suggested that anti-PD-1 therapy was less effective in most *TP53*-mutant patients with HNSCC.

We tested other chemotherapeutic and targeted drugs, and the results showed a difference between the predicted

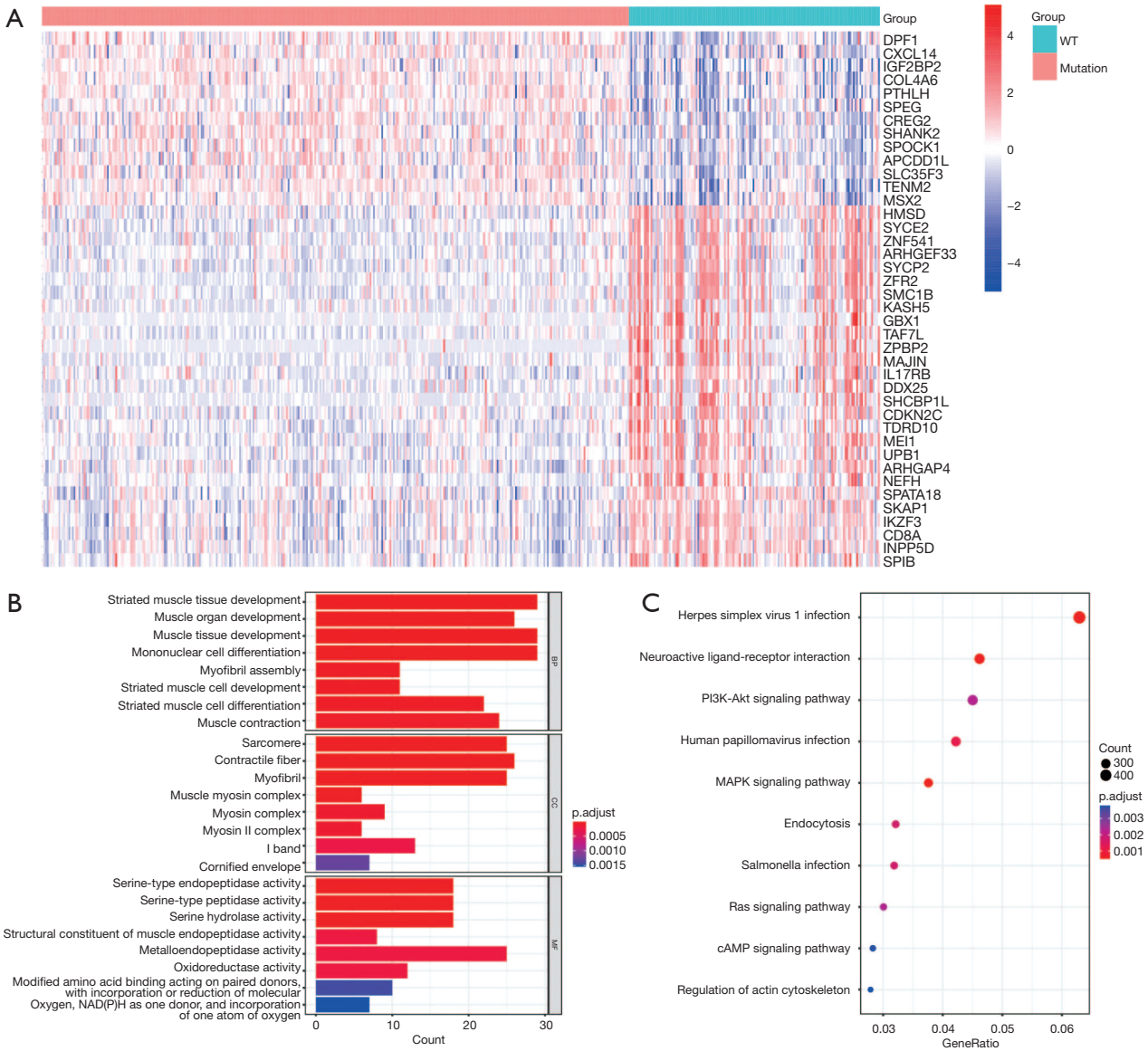

Figure 6 GO and KEGG enrichment analysis of *TP53* mutation-related DEGs in HNSCC based on TCGA database. (A) Heatmap showing the top 40 DEGs. (B) GO enrichment analysis of the enriched BPs, CC, and MF. (C) KEGG enrichment analysis. GO, Gene Ontology; KEGG, Kyoto Encyclopedia of Genes and Genomes; DEGs, differentially expressed genes; HNSCC, head and neck squamous cell carcinoma; TCGA, The Cancer Genome Atlas; BPs, biological processes; CC, cell composition; MF, molecular function; WT, wild-type.

value of IC_{50} for patients with *TP53*-mutant HSNCC and those with *TP53* wild-type HSNCC. *TP53*-mutant patients with HNSCC exhibited a higher sensitivity to camptothecin methotrexate, etoposide, bleomycin, lenalidomide, and rapamycin (P<0.001). Patients with HNSCC and *TP53* mutations were less sensitive to methotrexate, etoposide, bleomycin, lenalidomide, and rapamycin (*Figure 5E*).

Enrichment pathway analysis of TP53 mutation

To further clarify the difference between the *TP53*-mutant and wild-type group, the analysis of 501 HNSCC samples identified 403 DEGs, including 253 upregulated and 150 downregulated genes. We generated a hierarchical clustering heatmap to present the top 40 DEGs of each group (*Figure 6A*). We also performed GO and KEGG enrichment analyses to identify the most common

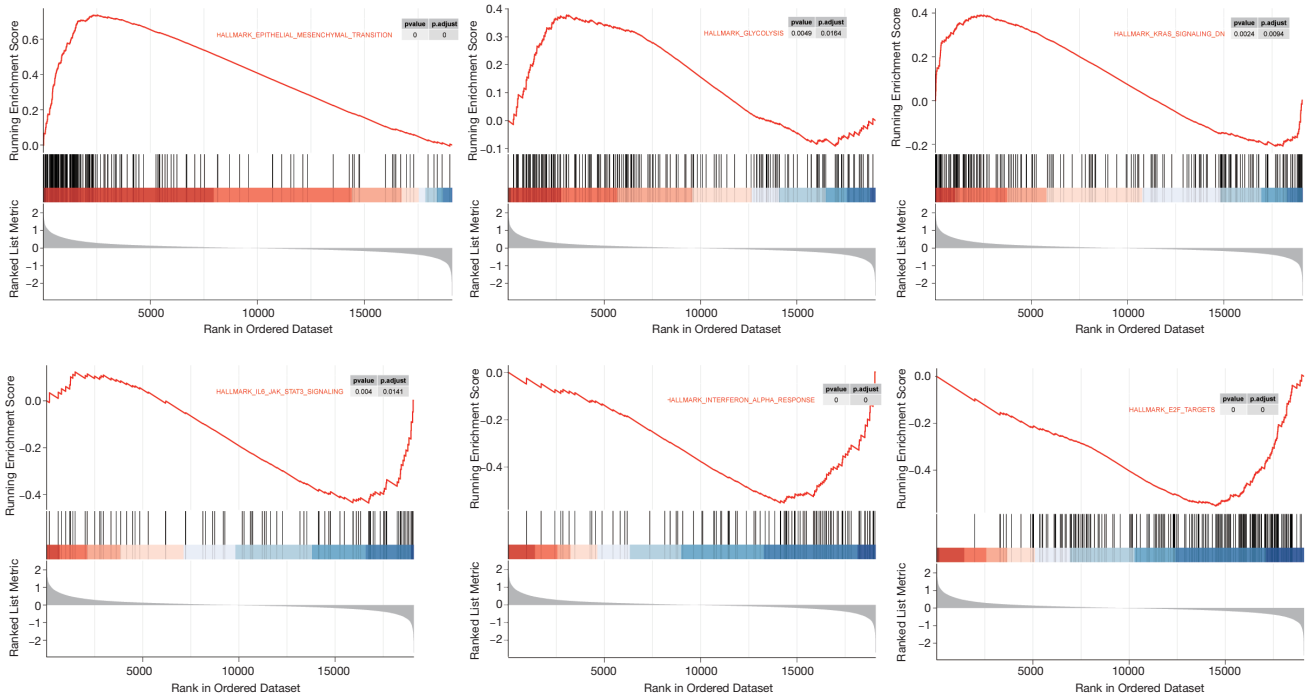

Figure 7 GSEA of *TP53* mutation-related DEGs based on TCGA database in HNSCC. GSEA, gene set enrichment analysis; DEGs, differentially expressed genes; TCGA, The Cancer Genome Atlas; HNSCC, head and neck squamous cell carcinoma.

biological processes and pathways involved in these DEGs. GO enrichment analysis showed that these DEGs were mainly enriched in striated muscle tissue development, structural constituent of muscle, and endopeptidase activity (*Figure 6B*), while the results of KEGG enrichment analysis indicated that these DEGs were primarily enriched in neuroactive ligand-receptor interaction, phosphatidylinositide 3-kinases/protein kinase B (PI3K–AKT) signaling pathway, MAPK signaling pathway, and endocytosis (*Figure 6C*). Furthermore, GSEA was performed based on the *TP53* mutation, and it showed that the *TP53* mutation could upregulate the signaling pathways involved in epithelial-mesenchymal transition, Kirsten rat sarcoma viral oncogene homolog (KRAS) upregulation, and the glycolysis pathway and downregulate signaling pathways involved in interleukin 6–Janus kinase–signal transducer and activator of transcription 3 (IL6–JAK–STAT3) signaling, interferon α response, and *E2F* targets (*Figure 7*).

Concordance between TP53 mutation identified in plasma cfDNA and matched HNSCC tissue DNA

Figure 8 illustrates the specific mutation spectrum and clinical characteristics of each of the nine sample pairs with mutations. The results showed that the mutation frequency of *TP53* was the highest among all mutated genes. In cfDNA samples, the mutation frequency of *TP53* was 66.67%. In matched tumor biopsy, *TP53* mutation was detected in all patients. Only 27.27% of the tissue tumor variants were detected outside of plasma when all *TP53* mutations were considered. *Table 2* depicts the detailed mutations of *TP53* in paired samples of cfDNA and tumor tissue.

Discussion

Certain studies indicate that *TP53* is a tumor suppressor that can inhibit the occurrence and development of tumors by regulating tumor proliferation, apoptosis, angiogenesis, and DNA repair (18,19). *TP53* mutations have been observed in various cancers and are correlated with reduced OS (20). In this study, *TP53* was the most frequently mutated gene in HNSCC. *TP53* mutation was also associated with HNSCC poor prognosis. Numerous studies have suggested that *TP53* mutations play a crucial role in tumor recognition and antitumor immune surveillance via the immune system (21,22). In our study, the *TP53*-mutant group showed lower immune and ESTIMATE scores, thereby suggesting poor prognosis, which was consistent with the poorer survival

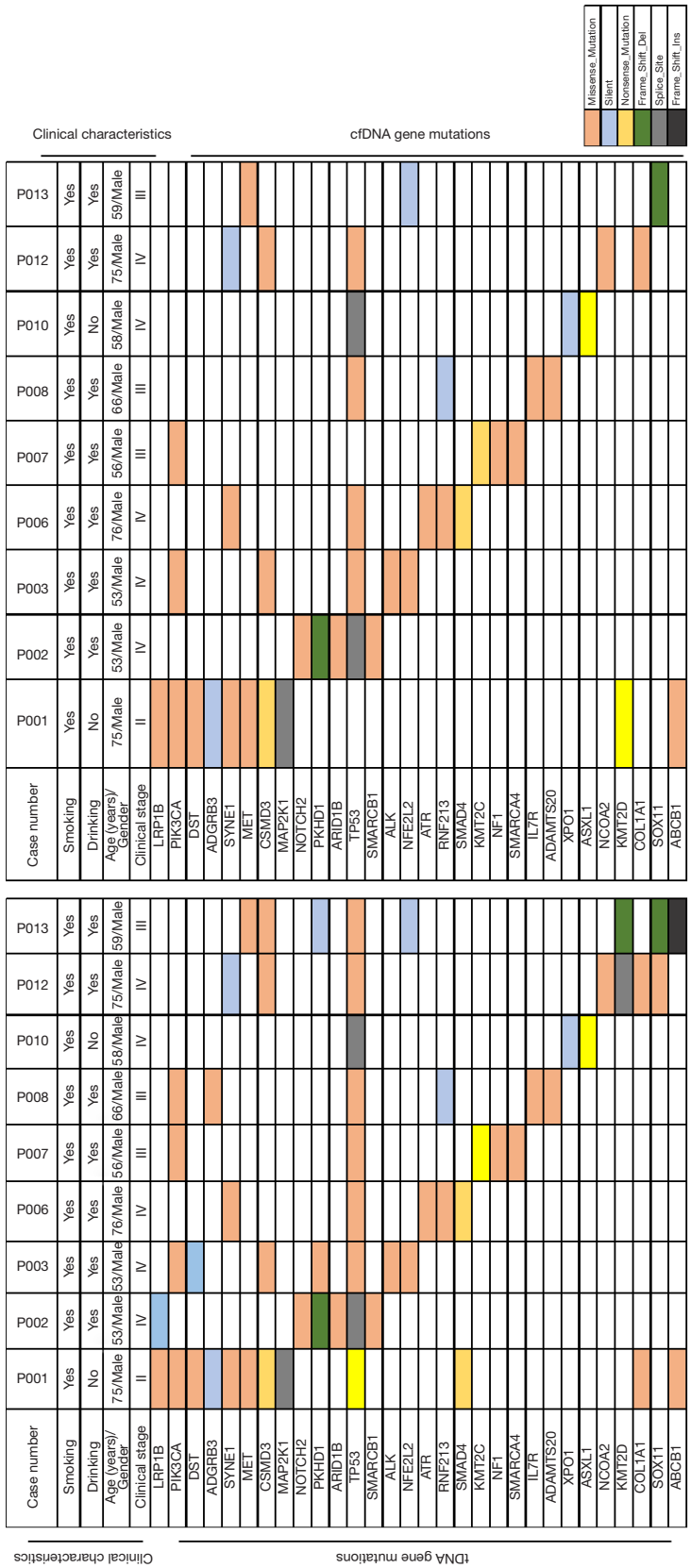

Figure 8 Somatic mutational landscape of nine cfDNA samples in tDNA and cfDNA. cfDNA, cell-free DNA; tDNA, tumor DNA.

Table 2 Details of *TP53* variants found in HNSCC patient-matched plasma cfDNA and tissue (n=9)

Sample ID	Gene	Variant class	Exon	AA change	COSMIC database	Variant detected in matched plasma cfDNA	AF in tumor (%)	AF in plasma (%)
P001	*TP53*	Nonsense mutation	Exon4	c.G484T	COSMIC	No	21	–
P002	*TP53*	Splice site	Exon4	c.559+1G>T	COSMIC	Yes	86.6	1.3
P003	*TP53*	Missense mutation	Exon4	c.G460A	COSMIC	Yes	19.8	1.8
P006	*TP53*	Splice site	Exon12	c.1101-2A>T	COSMIC	Yes	22.2	1.8
P006	*TP53*	Missense mutation	Exon4	c.G428T	COSMIC	Yes	18.4	1.3
P007	*TP53*	Missense mutation	Exon1	c.G128A	COSMIC	No	29.4	–
P008	*TP53*	Missense mutation	Exon6	c.A598T	NA	Yes	39.1	0.18
P008	*TP53*	Splice site	Exon11	c.994-1G>T	COSMIC	Yes	40.3	0.27
P010	*TP53*	Splice site	Exon6	c.559+1G>A	COSMIC	Yes	7.8	0.13
P012	*TP53*	Missense mutation	Exon4	c.G422A	COSMIC	Yes	34.6	0.88
P013	*TP53*	Missense mutation	Exon1	c.C56G	COSMIC	No	63.1	–

HNSCC, head and neck squamous cell carcinoma; cfDNA, cell-free DNA; AA, allele alteration; AF, allele frequency; NA, not applicable.

in the *TP53*-mutant group. Immune cell infiltration is an important feature of the tumor microenvironment. The *TP53*-mutant group exhibited higher CD56 bright NK cell infiltration than did the *TP53* wild-type group of patients with HSNCC. The levels of activated B cells, activated CD4 T cells, and eosinophils were markedly decreased in the *TP53*-mutant group. These results indicated that the *TP53*-mutant group was prone to immune escape.

PD-1 is an immune checkpoint that usually inhibits the antitumor immune responses of tumor cells by combining with PD-L1 (23). In our study, the level of PD-L1 in the *TP53*-mutant group was significantly lower than that in the *TP53* wild-type group, and the result was consistent across multiple databases (RNA-sequencing and RPPA). Previous studies have reported that p53 can enhance PD-L1 expression by regulating the loss of function of miR-34 (24,25). However, we did not find a positive correlation between miR-34 and *TP53* status in our study. We evaluated the potential clinical efficacy of immunotherapy in *TP53* mutations using TIDE. The higher the TIDE prediction score is, the higher the likelihood of immune evasion. The results showed a higher TIDE score in the *TP53*-mutant group, indicating that ICB has poor efficacy in patients with *TP53* mutations. We can easily predict the efficacy of ICB therapy in patients using TIDE, but the specific treatment effect and identification of biomarkers still need to be clarified by extensive clinical trials for verification.

Additionally, the sensitivity of the *TP53*-mutant group to chemotherapeutic and targeted drugs was explored. The data suggested that the use of camptothecin, methotrexate, etoposide, blemycin, lenalidomide, and rapamycin for those with *TP53* mutations may be effective.

According to the DEGs between the *TP53* mutation and wild-type groups, GSEA and GO and KEGG enrichment analysis were performed, and we found that the *TP53* mutation was associated with the glycolysis pathway in patients with HNSCC. This metabolic phenotype is characterized by a preferential reliance on glycolysis (the process by which glucose is converted to pyruvate and then lactate) to produce energy anaerobically (26). Glycolysis plays an important role in oncogenic regulation. Therefore, overcoming drug resistance by inhibiting the glycolysis in cancer cells is a novel strategy (27).

In this study, *TP53* mutations were detected in tissue and serum cfDNA derived from patients with HNSCC. As the cfDNA of tumor cells is released in the blood, the mutational status of cfDNA may reflect the genetic characteristics of the primary or metastatic lesions (28). In our study, only 27.27% of the tissue tumor variants were detected outside of cfDNA in a consideration of all *TP53* mutations. These results suggest that the *TP53* mutation in patients with HNSCC could be measured in serum DNA.

Conclusions

Our study further confirmed that *TP53* mutation in patients with HSNCC was associated with poor prognosis. We also explored the response of patients with *TP53*-

mutant patients with HNSCC to immunotherapies and chemotherapies. Furthermore, the detection of *TP53* mutations in serum-derived cfDNA from patients with HSNCC was demonstrated to be feasible. In the future, we may predict the prognosis and treatment of patients with HNSCC by detecting *TP53* mutations in cfDNA.

Acknowledgments

Funding: This study was supported by the Tianjin Key Medical Discipline Construction Project, the Tianjin Health Research Project (ZC20010); Tianjin Science and Technology Project (21JCQNJC01770, 21JCZDJC01200, 21JCQNJC01670, 21JCQNJC01780, and 21JCYBJC01570), and the Tianjin Health Research Project (TJSJMYXYC-D2-021).

Footnote

Reporting Checklist: The authors have completed the REMARK reporting checklist. Available at https://tcr.amegroups.com/article/view/10.21037/tcr-23-878/rc

Data Sharing Statement: Available at https://tcr.amegroups.com/article/view/10.21037/tcr-23-878/dss

Peer Review File: Available at https://tcr.amegroups.com/article/view/10.21037/tcr-23-878/prf

Conflicts of Interest: All authors have completed the ICMJE uniform disclosure form (available at https://tcr.amegroups.com/article/view/10.21037/tcr-23-878/coif). The authors have no conflicts of interest to declare.

Ethical Statement: The authors are accountable for all aspects of the work in ensuring that questions related to the accuracy or integrity of any part of the work are appropriately investigated and resolved. The study was conducted in accordance with the Declaration of Helsinki (as revised in 2013) and was approved by the independent ethics committee of Tianjin First Central Hospital (protocol no. 2020N115KY). Informed consent was obtained from all individual participants.

References

1. Johnson DE, Burtness B, Leemans CR, et al. Head and neck squamous cell carcinoma. Nat Rev Dis Primers 2020;6:92.
2. Sabatini ME, Chiocca S. Human papillomavirus as a driver of head and neck cancers. Br J Cancer 2020;122:306-14.
3. Mulder FJ, Pierssens DDCG, Baijens LWJ, et al. Evidence for different molecular parameters in head and neck squamous cell carcinoma of nonsmokers and nondrinkers: Systematic review and meta-analysis on HPV, p16, and TP53. Head Neck 2021;43:303-22.
4. Deneka AY, Baca Y, Serebriiskii IG, et al. Association of TP53 and CDKN2A Mutation Profile with Tumor Mutation Burden in Head and Neck Cancer. Clin Cancer Res 2022;28:1925-37.
5. Vitale SR, Sieuwerts AM, Beije N, et al. An Optimized Workflow to Evaluate Estrogen Receptor Gene Mutations in Small Amounts of Cell-Free DNA. J Mol Diagn 2019;21:123-37.
6. Nikanjam M, Kato S, Kurzrock R. Liquid biopsy: current technology and clinical applications. J Hematol Oncol 2022;15:131.
7. Lin D, Shen L, Luo M, et al. Circulating tumor cells: biology and clinical significance. Signal Transduct Target Ther 2021;6:404.
8. Lin D, Shen L, Luo M, et al. Circulating tumor cells: biology and clinical significance. Signal Transduct Target Ther 2021;6:404.
9. Jiang P, Gu S, Pan D, et al. Signatures of T cell dysfunction and exclusion predict cancer immunotherapy response. Nat Med 2018;24:1550-8.
10. Geeleher P, Cox N, Huang RS. pRRophetic: an R package for prediction of clinical chemotherapeutic response from tumor gene expression levels. PLoS One 2014;9:e107468.
11. Vanden Heuvel JP, Maddox E, Maalouf SW, et al. Replication Study: Systematic identification of genomic markers of drug sensitivity in cancer cells. Elife 2018;7:e29747.
12. de Jong A, Kuipers OP, Kok J. FUNAGE-Pro: comprehensive web server for gene set enrichment analysis of prokaryotes. Nucleic Acids Res 2022;50:W330-6.

13. Lydiatt WM, Patel SG, O'Sullivan B, et al. Head and Neck cancers-major changes in the American Joint Committee on cancer eighth edition cancer staging manual. CA Cancer J Clin 2017;67:122-37.
14. Shi C, Liu S, Tian X, et al. A TP53 mutation model for the prediction of prognosis and therapeutic responses in head and neck squamous cell carcinoma. BMC Cancer 2021;21:1035.
15. Chen Y, Li ZY, Zhou GQ, et al. An Immune-Related Gene Prognostic Index for Head and Neck Squamous Cell Carcinoma. Clin Cancer Res 2021;27:330-41.
16. Cortez MA, Ivan C, Valdecanas D, et al. PDL1 Regulation by p53 via miR-34. J Natl Cancer Inst 2015;108:djv303.
17. Song D, Lyu H, Feng Q, et al. Subtyping of head and neck squamous cell cancers based on immune signatures. Int Immunopharmacol 2021;99:108007.
18. Wang Z, Strasser A, Kelly GL. Should mutant TP53 be targeted for cancer therapy? Cell Death Differ 2022;29:911-20.
19. Tang Z, Zeng M, Wang X, et al. Synthetic lethality between TP53 and ENDOD1. Nat Commun 2022;13:2861.
20. Donehower LA, Soussi T, Korkut A, et al. Integrated Analysis of TP53 Gene and Pathway Alterations in The Cancer Genome Atlas. Cell Rep 2019;28:1370-1384.e5.
21. Nathan CA, Khandelwal AR, Wolf GT, et al. TP53 mutations in head and neck cancer. Mol Carcinog 2022;61:385-91.
22. Ganci F, Allegretti M, Manciocco V, et al. Two distinct TP53 mutations in HNSCC primary tumor: Only one circulates in the blood. Oral Oncol 2021;115:105096.
23. Yi M, Zheng X, Niu M, et al. Combination strategies with PD-1/PD-L1 blockade: current advances and future directions. Mol Cancer 2022;21:28.
24. Pan W, Chai B, Li L, et al. p53/MicroRNA-34 axis in cancer and beyond. Heliyon 2023;9:e15155.
25. Liu C, Rokavec M, Huang Z, et al. Curcumin activates a ROS/KEAP1/NRF2/miR-34a/b/c cascade to suppress colorectal cancer metastasis. Cell Death Differ 2023;30:1771-85.
26. Reinfeld BI, Rathmell WK, Kim TK, et al. The therapeutic implications of immunosuppressive tumor aerobic glycolysis. Cell Mol Immunol 2022;19:46-58.
27. Paul S, Ghosh S, Kumar S. Tumor glycolysis, an essential sweet tooth of tumor cells. Semin Cancer Biol 2022;86:1216-30.
28. van Dessel LF, Vitale SR, Helmijr JCA, et al. High-throughput isolation of circulating tumor DNA: a comparison of automated platforms. Mol Oncol 2019;13:392-402.

Cite this article as: Wei M, Zhi J, Li L, Wang W. Predicting therapeutic responses in head and neck squamous cell carcinoma from *TP53* mutation detected by cell-free DNA. Transl Cancer Res 2023;12(12):3604-3617. doi: 10.21037/tcr-23-878

